ELSEVIER

One-dimensional simulation model for steady transcritical free surface flows at short length transitions

Yebegaeshet T. Zerihun [a,*], John D. Fenton [b]

[a] *Department of Civil and Environmental Engineering, University of Melbourne, Victoria 3010, Australia*
[b] *School of Anthropology, Geography, and Environmental Studies, University of Melbourne, Victoria 3010, Australia*

Abstract

A numerical experiment is carried out to investigate the suitability of a Boussinesq-type momentum model for simulating transcritical flows at short length transitions in open channel flow measuring structures. Two one-dimensional Boussinesq-type equation models, which incorporate different degrees of dynamic pressure corrections, are considered for this purpose. A finite difference method is employed to discretise and solve the equations. The models are then applied to simulate different test cases for flows in such channels with predominant non-hydrostatic pressure distribution effects. A comparison of the computed results with the corresponding experimental data is presented. Results of this study reveal that the proposed model, which includes a higher-order correction for the effect of the centrifugal pressure, describes well even relatively abrupt changes from sub- to super-critical flow state.
© 2005 Published by Elsevier Ltd.

Keywords: Open channel flow; Hydrodynamics; Boussinesq equation; Non-uniform flow

1. Introduction

In most open channel flow measuring structures such as venturi flumes, the geometries of both the sidewalls and the bed vary along the direction of the flow. It is well-known that such geometric changes result in flow transition from subcritical to supercritical state under free flow conditions. The major characteristic of the flow in the vicinity of such short length transition is a strong departure from the hydrostatic distribution of pressure caused by the curvatures of the streamlines. Common computational flow models, which assume hydrostatic pressure distribution, cannot describe such types of flows. The essential vertical details of the flows require the use of more accurate methods for description of such flow situations. In this study, a one-dimensional model that incorporates a correction for the effect of the centrifugal dynamic pressure due to the

curvature of the streamline will be employed for the numerical simulation of free flow in such types of flow measuring structures.

Flow problems related to open channel flow measuring structures have been extensively studied experimentally. Most of the experimental works were performed to understand the flow characteristics of these structures as well as the determination of the coefficients of discharge (see e.g., [2]). Compared to previous simulation studies of flow over a sill, however, free flows in venturi flumes with and without humps have not been thoroughly investigated numerically using a one-dimensional higher-order equation. In such flumes with short constrictions, the combined effects of the variation of the sidewalls and bed geometries predominantly affect the behaviour of the transcritical flows particularly in the transition region. In this region, the flows exhibit three-dimensional characteristics with cross-waves that influence the configuration of the downstream (supercritical flow region) flow profile. From a practical perspective, accurate simulation of the upstream

---

* Corresponding author.
  E-mail address: y.zerihun@civenv.unimelb.edu.au (Y.T. Zerihun).

Notation

A	flow cross-sectional area	x	horizontal coordinate
B	width of the channel	y	transverse coordinate
Fr	Froude number	z	vertical coordinate
g	acceleration due to gravity	Z_b	channel bed elevation
h	step size in the horizontal direction	Z_b', Z_b'', Z_b'''	derivatives of the bed profile
h_s	height of a point in the flow field above the bed	α	angle of inclination to the horizontal
H	depth of flow measured vertically from the bed	β	Boussinesq coefficient
H_1	total energy head over the crest of the weir	δH_j	correction depth at node j
L_w	crest length of the weir	η	mean elevation of the free surface
m	total number of nodal points in the solution domain	κ	curvature of a streamline
		κ_b	curvature of the bed
p	pressure	κ_H	curvature of the flow surface
p_0	hydrostatic pressure at the bed	ξ	non-linear term associated with the flow equation
Q	discharge		
S_f	friction slope	ρ	density of the fluid
S_H	slope of the flow surface	ω_0	a weighting factor
S_0	slope of the bed		

water surface elevation and/or piezometric head is important in order to predict the discharge capacity of these structures.

Several investigations have been performed in the past to model flow situations that involve non-hydrostatic pressure distribution effects, using different approaches. Boussinesq [3] was the first to extend the momentum equation to incorporate implicitly the effect of curvature of the streamlines using the assumption of a linear variation of curvature of streamlines from the bed to the free surface. Recently, Dressler [4], Hager and Hutter [7], Hager [8] and Matthew [14] have developed higher-order equations to model two-dimensional flow problems. Similar to the Boussinesq [3] equation, however these equations are limited to the solution of irrotational flow problems only. For fast flow over the chute part of a hydraulic structure such as a spillway, the assumption of irrotational flow, which was the basis of all these governing equations, is questionable. It has also been shown in different studies (see e.g., [5,17]) that the Dressler equations do not permit flow regime to change from subcritical to supercritical state. Steffler and Jin [18] developed the vertically averaged and moment (VAM) equations based on the assumptions of a linear longitudinal velocity distribution, and quadratic pressure and vertical velocity distributions across the depth of flow. However, the resulting equations are long and complex. Khan and Steffler [10,11] studied the applicability of the VAM equations.

Fenton [5] introduced alternative equations to model flow problems with appreciable curvature of streamline. He used the momentum principle along with the assumption of a constant centrifugal term, $\kappa/\cos\alpha$ ($\kappa =$ curvature and $\alpha =$ angle of inclination of the streamline with the horizontal axis), at a vertical section to develop the equa-

tions. The vertical distribution of this term determines the degree of the resulting correction factor for the effects of the streamline curvature. Compared to other governing equations (for instance, Dressler and VAM equations), the equations are simple to apply in a cartesian coordinate system especially for flow problems with continuous flow boundaries. In this work, these equations along with the modified version, which are developed based on the assumption of a linear variation of centrifugal term with depth, are investigated for simulating steady transcritical flow situation with short length of transitions in open channel flow measuring structures. These include free flows over trapezoidal profile weirs as well as in venturi flumes with and without humps, and free overfall in a rectangular channel. The study also aims to assess systematically the impact of the pressure correction factors on the simulation of pressure and flow surface profiles of such flows.

In the following sections the governing equations are presented and the main features of the computational model, namely the spatial discretisation of the equations and the solution procedure for the resulting non-linear discretised equations are outlined. The inclusion of the boundary conditions in this procedure is also discussed. The results of the simulation for several steady flow test cases are verified by comparing them with experimental data.

2. Governing equations

As discussed above, Fenton [5] presented a simple method that incorporates the possible variation of the width of the channel. For steady flow in a rectangular channel, this method yields the following equations:

$$\beta \frac{Q^2 H}{4A} \frac{\mathrm{d}^3 H}{\mathrm{d}x^3} + \beta \frac{Z_{\mathrm{b}}' Q^2}{2A} \frac{\mathrm{d}^2 H}{\mathrm{d}x^2}$$
$$+ (1 + Z_{\mathrm{b}}'^2)\left(\left(gA - \beta \frac{Q^2 B}{A^2}\right)\frac{\mathrm{d}H}{\mathrm{d}x} + gA(Z_{\mathrm{b}}' + S_{\mathrm{f}})\right)$$
$$+ \omega_0 \beta \frac{HQ^2}{A}\left(\frac{Z_{\mathrm{b}}'''}{2} + \frac{Z_{\mathrm{b}}' Z_{\mathrm{b}}''}{H}\right)$$
$$- \beta \frac{HQ^2}{A^2}\left((1 + Z_{\mathrm{b}}'^2) + H\left(\frac{1}{2}\frac{\mathrm{d}^2 H}{\mathrm{d}x^2} + \omega_0 Z_{\mathrm{b}}''\right)\right)\frac{\mathrm{d}B}{\mathrm{d}x} = 0, \tag{1}$$

$$p = \rho(\eta - z)\left(g + \frac{\beta Q^2}{A^2(1 + Z_{\mathrm{b}}'^2)}\left(\omega_0 Z_{\mathrm{b}}'' + \frac{1}{2}\frac{\mathrm{d}^2 H}{\mathrm{d}x^2}\right)\right), \tag{2}$$

in which H is the depth of flow; $Z_{\mathrm{b}}^{P'}$, Z_{b}'' and Z_{b}''' are the first, second and third derivatives of the bed profile respectively; S_{f} denotes the friction slope, calculated from the Manning equation or smooth boundary resistance law; Q is the discharge; A is flow cross-sectional area; B is the width of the channel; β refers to the Boussinesq coefficient; g is gravitational acceleration; ρ is the density of the fluid; η is the mean elevation of the free surface; z is the vertical coordinate of a point in the flow field; p is the pressure; and ω_0 is a weighting factor. Fenton [5] suggested a value of slightly less than 1 for ω_0. These Eqs. (1) and (2), will be referred to hereafter as the Boussinesq-type momentum equation with uniform centrifugal term (BTMU) model. Following the procedures suggested by Fenton [5] and assumption of a *linear* variation of the centrifugal term with depth, the following equations are developed for steady flow in a rectangular channel:

$$\frac{Q^2 H}{3A} \frac{\mathrm{d}^3 H}{\mathrm{d}x^3} + \frac{Q^2 Z_{\mathrm{b}}'}{2A} \frac{\mathrm{d}^2 H}{\mathrm{d}x^2}$$
$$+ \left(gA - \beta \frac{Q^2 B}{A^2}\right)\frac{\mathrm{d}H}{\mathrm{d}x} + gA(Z_{\mathrm{b}}' + S_{\mathrm{f}}) + \frac{HQ^2}{A}\left(\frac{Z_{\mathrm{b}}'''}{2} + \frac{Z_{\mathrm{b}}' Z_{\mathrm{b}}''}{H}\right)$$
$$- \frac{H^2 Q^2}{A^2}\left(\frac{\beta}{H} + Z_{\mathrm{b}}'' + \frac{2}{3}\frac{\mathrm{d}^2 H}{\mathrm{d}x^2}\right)\frac{\mathrm{d}B}{\mathrm{d}x} = 0, \tag{3}$$

$$p = \rho\left(g(\eta - z) + \frac{Q^2}{A^2}\left(Z_{\mathrm{b}}''(\eta - z) + \frac{\mathrm{d}^2 H}{\mathrm{d}x^2}\left(\frac{\eta - z}{\eta - Z_{\mathrm{b}}}\right)\right.\right.$$
$$\left.\left. \times \left(\frac{1}{2}(\eta + z) - Z_{\mathrm{b}}\right)\right)\right). \tag{4}$$

These equations in this paper are termed the Boussinesq-type momentum equation linear (BTML) model. In the formulation of both models, the curvature at the surface is approximated by $\kappa_H \cong \mathrm{d}^2 H/\mathrm{d}x^2 + Z_{\mathrm{b}}''$ and at the bed by $\kappa_{\mathrm{b}} \cong Z_{\mathrm{b}}''$. If Eq. (4) is compared with the corresponding equation, Eq. (2), it is noticed that the term which accounts for the dynamic effect due to the curvature of the flow surface shows a quadratic variation in Eq. (4). It should be remarked that Eq. (2) predicts a linearly varying non-hydrostatic pressure distribution. In this work, the two models will be applied to simulate transcritical flows over curved beds with and without lateral contractions. The simulation results of the two models will be compared with

measurements to examine the influence of the pressure correction factors on the solutions of the models.

3. Problem formulation and boundary conditions

The computational domain for the numerical solution of the flow problem is shown in Fig. 1. In this figure AB and CD are the inflow and outflow sections respectively, and BD is the curved flow boundary. The inflow and outflow sections of the computational domain are located in a region where the flow is assumed to be nearly uniform, with hydrostatic pressure distribution. This quasi-uniform flow condition simplifies the evaluation of the boundary values at these sections using the gradually-varied flow equation,

$$S_H = \frac{\mathrm{d}H}{\mathrm{d}x} = \frac{S_0 - S_{\mathrm{f}}}{1 - \beta Fr^2}, \tag{5}$$

where Fr is the Froude number and S_0 is the bed slope. From this, for given depth and discharge at the inflow section, the corresponding slope of the water surface S_H, can be evaluated numerically. For given boundary values at the inflow and outflow sections, and discharge at the inflow section, it is required to determine the flow surface profile, AC, and the bed pressures along the flow boundary BD. For this purpose, the computational domain of the flow problem is discretised into equal size steps in x as shown in Fig. 1.

4. Computational model development

Numerical solution is necessary since closed-form solutions are not available for these non-linear differential equations. Finite difference approximations are used here for their solution. This formulation is simple to code and extensively used to solve linear or non-linear differential equations. For the purpose of discretisation, Eqs. (1) and (3) can be represented by a simple general equation as

$$\frac{\mathrm{d}^3 H}{\mathrm{d}x^3} + \xi_0 \frac{\mathrm{d}^2 H}{\mathrm{d}x^2} + \xi_1 \frac{\mathrm{d}H}{\mathrm{d}x} + \xi_2 + \xi_3 = 0, \tag{6}$$

where ξ_0, ξ_1, ξ_2 and ξ_3 are the non-linear coefficients associated with the model equation and the corresponding expressions can be obtained by comparing this equation
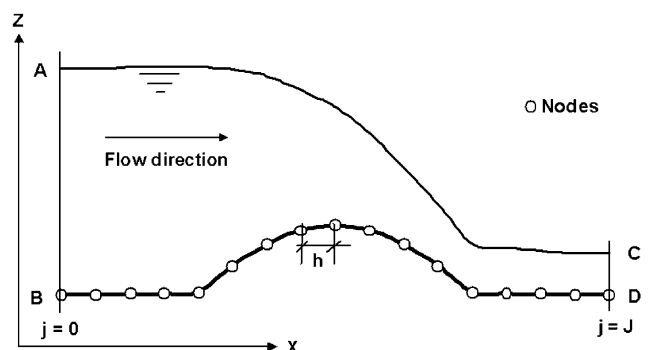

Fig. 1. Computational domain for transcritical flow problem.

with the respective flow equations. Higher-order finite difference approximations are employed to replace the derivative terms in these third-order differential equations in order to reduce the truncation errors introduced in the formulation due to the finite difference quotients (see e.g., [6]).

Upwind finite difference approximations [1] for derivatives at node j in terms of the nodal values at $j-2$, $j-1$, j and $j+1$ are introduced into Eq. (6). After simplifying the resulting expression and assembling similar terms together, the equivalent finite difference equation becomes

$$
\begin{aligned}
&6\xi_{2,j}h^3 + H_{j-2}(-6 + \xi_{1,j}h^2) + H_{j-1}(18 + 6\xi_{0,j}h - 6\xi_{1,j}h^2) \\
&\quad + H_j(-18 - 12\xi_{0,j}h + 3\xi_{1,j}h^2) \\
&\quad + H_{j+1}(6 + 6\xi_{0,j}h + 2\xi_{1,j}h^2) \\
&\quad - \frac{6h^3\mu_1}{B_j}\left(\frac{dB}{dx}\right)\left(\frac{\varphi_j}{H_j} + \frac{\mu_2}{h^2}(H_{j-1} - 2H_j + H_{j+1}) + \mu_3 Z''_{b,j}\right) \\
&= 0,
\end{aligned}
\tag{7}
$$

where h is the step size, and μ_1, μ_2 and μ_3 are constants related to the model equations and are given in Table 1. Since the value of the nodal point at $j = 0$ is known, the value of the imaginary node at $j = -1$ can be determined from the estimated water surface slope, S_H, at the inflow section. Using a similar discretisation equation for the water surface slope at inflow section and the expanded form of Eq. (7) at $j = 0$, the explicit expression for the nodal value at $j = -1$ in terms of values of the nodal point 0 and 1 is

$$
\begin{aligned}
H_{-1} = \left(\frac{-1}{\Omega + 6\Pi}\right)&(H_1\theta + H_0\Psi \\
&+ \Pi(6hS_H - 3H_0 - 2H_1) + 6\xi_{2,0}h^3),
\end{aligned}
\tag{8}
$$

where

$$
\theta = 6 + 6\xi_{0,0}h + 2\xi_{1,0}h^2;
$$
$$
\Psi = -18 - 12\xi_{0,0}h + 3\xi_{1,0}h^2;
$$
$$
\Omega = 18 + 6\xi_{0,0}h - 6\xi_{1,0}h^2; \quad \Pi = -6 + \xi_{1,0}h^2.
$$

Eqs. (7) and (8) constitute the one-dimensional finite difference scheme corresponding to the third-order ordinary differential equation, which is to be solved as a two-point boundary value problem. Generally, such problems must be solved by iterative methods, which proceed from an assumed initial free surface position. For the iterative procedure, the required computational effort is dependent on the choice of the initial flow surface profile. In this work, the Bernoulli and continuity equations are employed to obtain the initial flow surface profile estimate. Then, to simulate the flow surface profile, Eq. (7) is applied at different nodal points within the solution domain and results in a

sparse system of non-linear algebraic equations. These equations together with Eq. (8), and the two boundary values at the inflow and outflow sections, are solved by the Newton–Raphson iterative method with a numerical Jacobian matrix. The convergence of the solution is assessed using the following criterion:

$$
\left(\sum_{j=1}^{m}|\delta H_j| \bigg/ \sum_{j=1}^{m} H_j\right) \leqslant \text{tolerance},
$$

where δH_j is the correction depth to the solution of the nodal point j at any stage in the iteration; m is the total number of nodes in the solution domain excluding nodes having known values. In this study, a tolerance of 10^{-6} is used for the convergence of the numerical solution. The above described computational scheme is superior to the method employed by Fenton [5] which was based on the shooting technique and showed parasitic numerical instability.

For the solution of the pressure equations, a similar finite difference approximation is inserted into Eqs. (2) and (4) to discretise the derivative term in the equations. Since the nodal flow depth values are known from the solution of the flow profile equations, these discretised equations yield the bed pressure (for $z = Z_b$, where Z_b is the channel bed elevation) at different nodal points.

5. Simulation results and discussion

The steady one-dimensional flow models, presented in the previous section, were used for simulating: (i) transcritical flow over trapezoidal profile weirs; (ii) free flow in venturi flumes; (iii) transcritical flow over a curved bed combined with sidewall curvature; and (iv) a free overfall in a rectangular channel with subcritical approach flow. Experiments were performed for all cases in plexiglass laboratory flumes, and a smooth boundary resistance law was used to estimate the friction slope for the models. For computational simplicity, β was assumed as unity in both models.

For each test case, the influence of step size refinement on the solutions of the models was assessed for step sizes 20 mm, 25 mm, 30 mm, 50 mm and 100 mm. Due to space limitation only the results of the BTML model for free flow over a trapezoidal profile weir with $H_1/L_w = 0.79$ ($H_1 =$ total energy head over the weir crest, $L_w =$ weir crest length) are depicted in Fig. 2. When the step size exceeded 30 mm, the solutions of the models were affected by the discretisation errors. The finest discretisation ($h < 30$ mm) gave good flow profile simulation results without any surface undulation in the upstream subcritical flow region. As the discretisation became coarser, the models slightly underestimated the flow surface profile in the supercritical flow region. At the coarsest discretisation considered, however the bed pressure profile prediction was significantly affected.

Table 1
Values of the constant parameters for the model equations

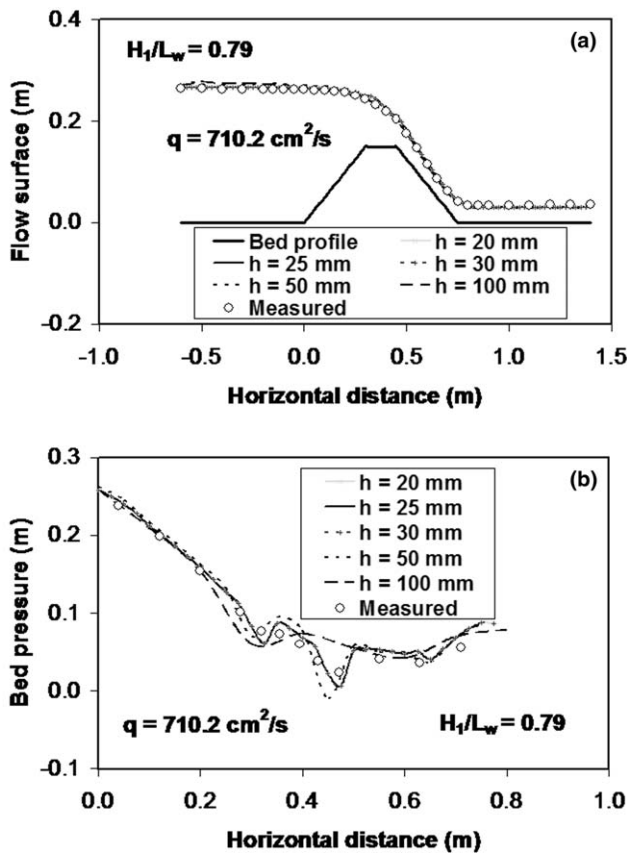| Model	μ_1	μ_2	μ_3	φ
BTMU equations	4	1/2	ω_0	$1 + Z'^2_b$
BTML equations	3	2/3	1	1

Fig. 2. Comparison of predictions for various step sizes: (a) flow surface profile; (b) bed pressure.

Accordingly, the computations for all simulation results presented in this paper were carried out using a uniform spatial step size of 20 mm.

5.1. Flow over trapezoidal profile weirs

Experiments on flow over trapezoidal profile weirs were conducted to validate the results of the models at the Michell Laboratory of the University of Melbourne, Australia. The flume was 7100 mm long, 380 mm deep, and 300 mm wide. The flume and the trapezoidal profile weirs were made of plexiglass. Water was supplied to the head tank from a sump through 115 mm diameter pipe with a valve for controlling the discharge. Various flow improving elements were provided upstream of the trapezoidal profile weirs to obtain a smooth flow without large-scale turbulence. Symmetrical trapezoidal profile weirs of 150 mm height, crest lengths 100 mm, 150 mm and 400 mm respectively, and side slope 1V:2H were tested at different discharges. The general set-up of the experiment is shown in Fig. 3.

A volumetric tank system was used to measure the discharge. The system consisted of a tank with plan dimensions of 200 cm by 150 cm and depth of 450 cm, and an inclined manometer (56.62° to the horizontal) for water
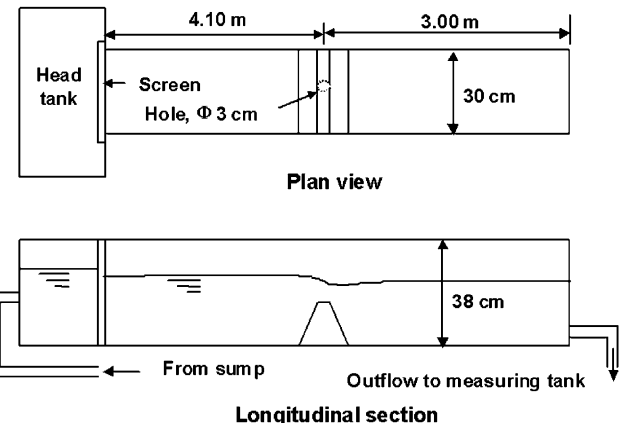

Fig. 3. Experimental set-up for flow over a trapezoidal weir.

level measurement in the tank. Tank filling time longer than 1 min was used to minimise errors associated with the starting and stopping of the stopwatch. The longitudinal flow surface profile was observed with a manual point gauge of reading accuracy 0.10 mm. For recording the bed pressure, steel pressure taps of external diameter 3 mm were fixed along the centreline of the weir model with maximum horizontal spacing of 80 mm, but the spacing was much closer near the edges of the weir crest. These pressure
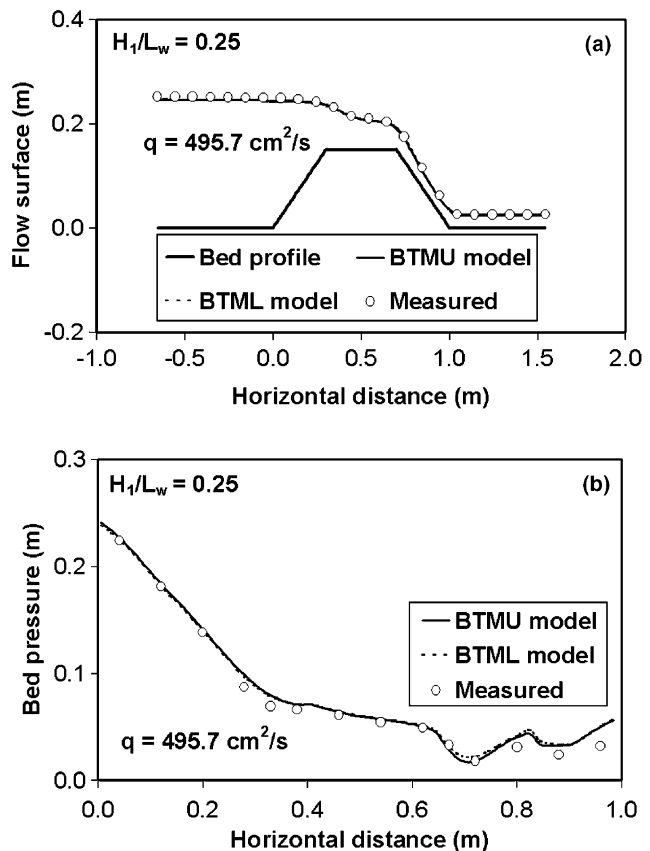

Fig. 4. Flow surface and bed pressure profiles for flow over a broad-crested weir.

taps were connected to vertical water piezometers of reading accuracy 1 mm by long plastic tubes that passed through a hole at the centreline of the flume bed. For each experiment, the base reading for the pressure taps was obtained immediately after the flow was shut off. According to the criteria given by Ranga Raju et al. [16], the effects of viscosity and surface tension on the experimental results were negligible.

For assessing the effect of the streamline curvature on the solution of the models, transcritical flow over such weirs with different H_1/L_w values were considered. The computed flow surface and bed pressure profiles for this flow situation are compared with experimental results in Figs. 4 and 5. The BTMU and BTML models solutions for flow surface profile show excellent agreement with the measured data, with maximum errors in the simulated flow profiles of only 1%. Both models predict similar flow surface profiles and steep flow surface slope on the crest of a short-crested weir. A minor discrepancy between the results of the two models for bed pressure profiles can be seen from these figures. In general, the overall qualities of the numerical solutions of the bed pressure are good and show good agreement with the experimental data (mean errors = 3.6% and 4% for the BTML and BTMU models, respectively). It is important to note that the observed bed pressure particularly in the downstream supercritical flow region might have some systematic errors due to turbulence effects.

5.2. Free flow in venturi flumes

5.2.1. Ye and McCorquodale's [19] experiment

Ye and McCorquodale [19] carried out an experiment in a Parshall flume model at the University of Windsor. This flume consisted of three sections: a converging inlet section with a horizontal bed and variable widths to create the critical depth; a throat section with parallel sidewalls and a sloping bed in which supercritical flow occurred; and a diverging outlet section with an adverse sloping bed and variable widths. Results for the flow surface profile measurements from this test were used for the verification of the model solutions.

Fig. 6 shows the computational results from the two flow models for transcritical flow in a Parshall flume. This figure compares the cross-channel averaged experimental and numerically predicted flow surface profiles along the centreline of the flume. The two models accurately simulate the flow transition from sub- to super-critical state for this flow condition. For the upstream flow region ($x \leqslant 0.8$ m), the agreement between the experimental and numerical results is good, and no significant differences are observed between the computational results of the two models over the entire flow region. However, a minor discrepancy between the models and experimental results can be seen from this figure in the supercritical flow region downstream of the diverging section of the flume ($x > 0.8$ m). In this flow region, the models slightly underestimate the flow surface elevation. As a one-dimensional model, these models do not describe the existence of cross-waves downstream of the end of the throat section.

5.2.2. Khafagi's [9] experiment

The experimental results of Khafagi [9] are invoked to test the ability of the model to simulate transcritical flow in a venturi flume. The test flume with horizontal bed consisted of three sections: a converging inlet section with a
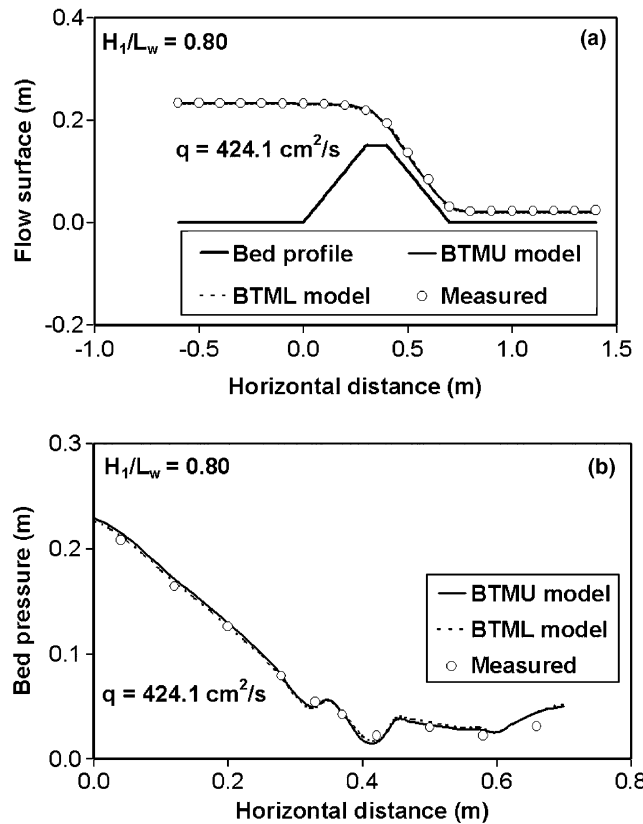

Fig. 5. Flow surface and bed pressure profiles for flow over a short-crested weir.
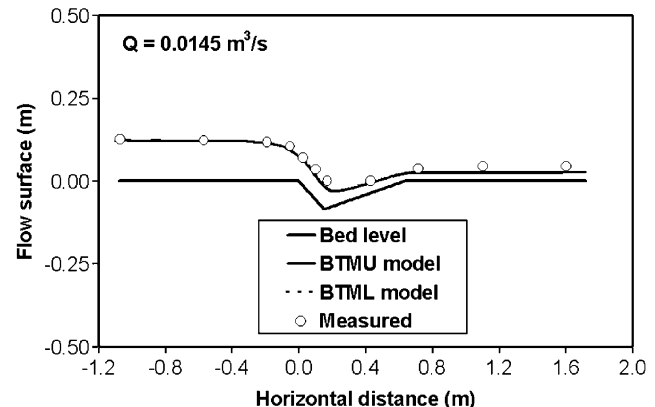

Fig. 6. Comparison of computational and experimental results for flow in a Parshall flume.

rounded constriction (radius = 545 mm) to create critical depth; a short throat section with parallel sidewalls; and a diverging outlet section (side slope 1:8) with a gradually varied width. The uncontracted width of the flume was 300 mm. The flow surface and pressure profiles measurements of different tests were used to validate the numerical models. Fig. 7 shows comparisons between measured and computed flow surface profiles along the centreline of the flume for transcritical flow with supercritical outflow condition downstream of the throat section. It can be seen from this figure that the two models simulate similar flow surface profiles for the entire flow region which agree very well with the experimental data. In both cases, the flow transition is accurately simulated.

In order to examine the influence of the applied corrections for the effect of the dynamic pressure in the simulation of local flow characteristics, the pressure distributions at the end of the converging ($x = 30$ cm) and at the beginning of the diverging ($x = 35$ cm) sections of the flume were simulated using these models. Fig. 8 shows the comparison of the experimental data and the numerical predictions of these models for the pressure distributions. In this figure the non-dimensional pressure distribution at a section, p/p_0 (p = pressure at height, h_s, above the bed, $p_0 = \rho g H$) is shown versus the non-dimen-

sional height above the bed, h_s/H. In both cases of pressure distribution simulations, the results of the BTML model show a slightly better agreement with measurements than the predictions of the BTMU model. The maximum differences between the experimental data and the corresponding numerically simulated values for the BTML and BTMU models are only 3.3% and 5.9%, respectively.

5.3. Flow in a channel with curved bed and sidewall

The results of the experiments conducted by Law [12] were selected to test the predictions of the models. A 16 m long recirculating glass wall flume was used to conduct the experiment. An obstacle made of plexiglass was installed at the middle of the flume to bring on simultaneous geometric changes in the bottom and sidewall of the flume. Due to this obstacle, the width of the channel was reduced to a minimum of 94 mm and the bed was elevated to a maximum height of 63 mm. The staggered distance between the maximum contraction and the maximum height of the hump was 200 mm. A point gauge of reading accuracy 0.30 mm was used to observe the flow profiles at the middle of the cross-section. Further details of the experimental set-up and procedures are given in Law [12].

A numerical simulation result based on the shooting method was reported by Law [13] for this flow problem.
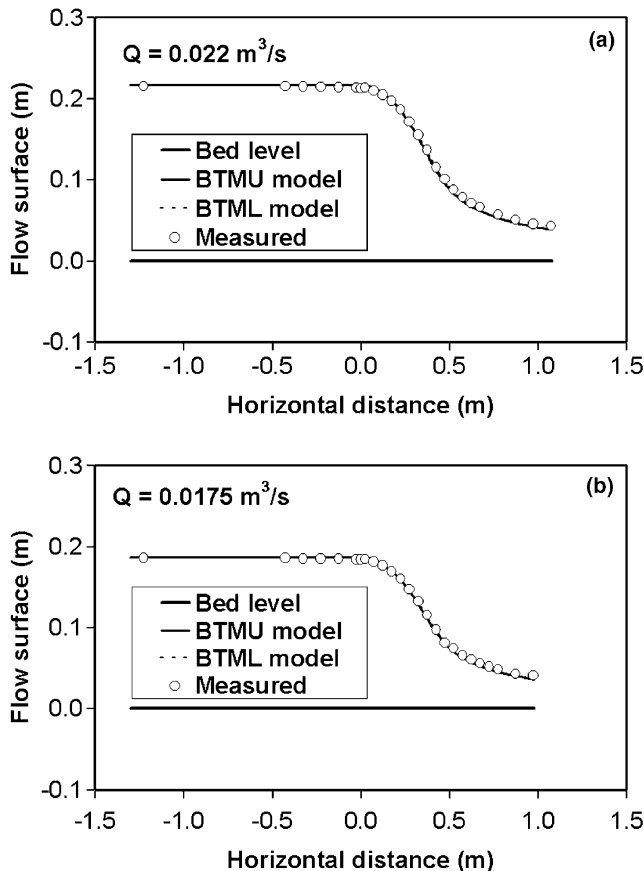

Fig. 7. Comparison of predicted and measured flow surface profiles for free flow situation.
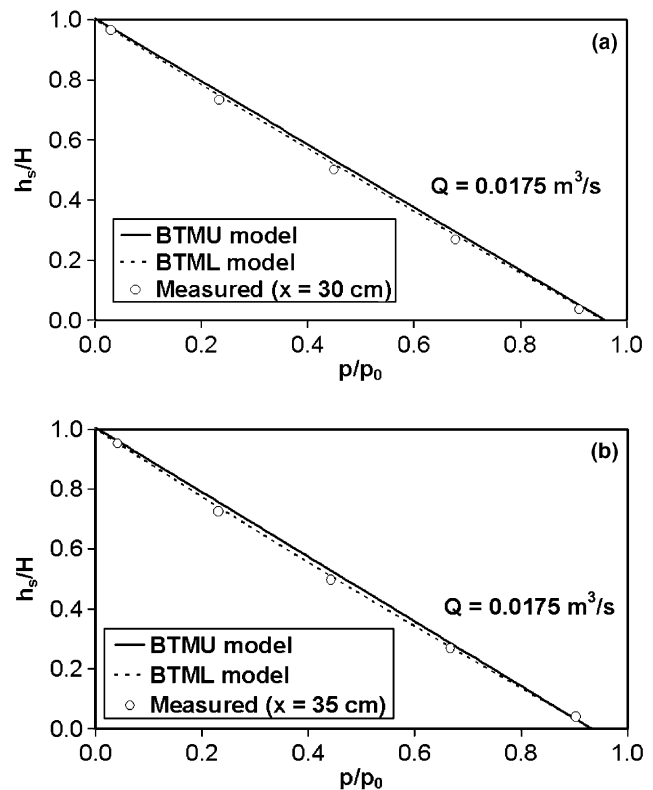

Fig. 8. Comparison of computational and experimental results for pressure distributions.

Similar to the Fenton [5] solution, however, Law's simulation result suffered from strong parasitic numerical instability besides the effects of bed profile discontinuity. In this work, smooth transition curves at both ends of the hump were introduced for smoothing the existing discontinuities.

Fig. 9 shows the comparison of the experimental data with the numerical predictions of the models for low and high flow cases. In the flow regions upstream of the minimum width of the flume ($x < 0$) and downstream of the maximum height of the hump, the BTML and BTMU models simulate similar flow profiles for both flow cases and are in good agreement with measurements. However, some differences are observed between the solutions of these models in the transition region where the combined effects of the curvatures of the bed and sidewall are substantial. In this region ($0 \leqslant x \leqslant 0.20$ m), the performance of the BTML model (maximum error = 1.8%) is marginally better than the BTMU model (maximum error = 3.5%). As can be seen from this figure, the predictions of these models slightly depart from measurements for high flow condition. This is probably due to the influence of the horizontal curvature of the streamline which is more significant in the transition region especially at higher discharge.
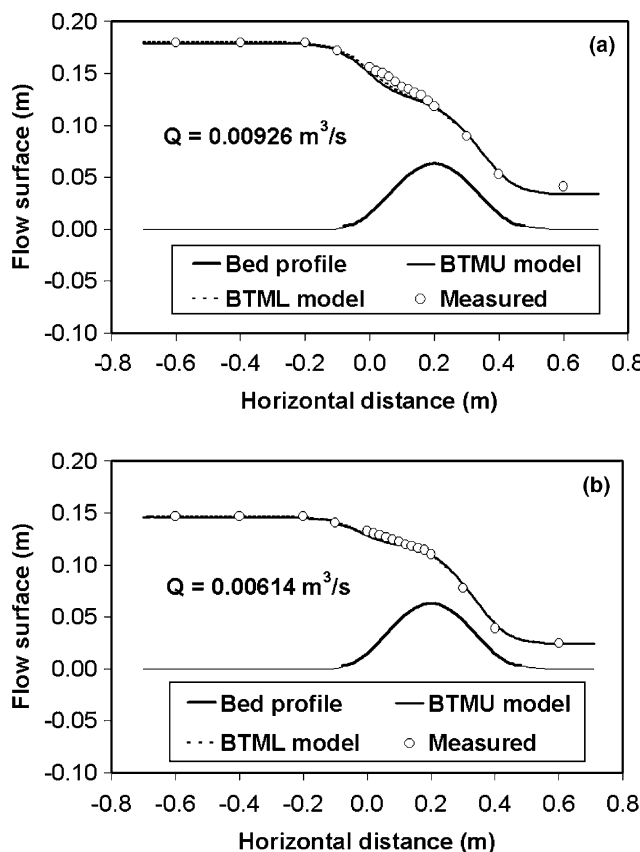
5.4. Free overfall simulation

The experimental data, consisting of flow depth and pressure distributions, for a free overfall in a rectangular channel were obtained from Rajaratnam and Muralidhar [15]. The experiments were performed in a plexiglass flume 457 mm wide, 381 mm deep and 6.1 m long. Flow surface profiles and pressure distributions at different sections up to the upstream control sections were measured for a few runs of these experiments. The results of run 1A were used for validating the prediction of the proposed models.

This test case was first presented by Khan and Steffler [11] who used the one-dimensional VAM equations and obtained results that are in good agreement with experimental data. In this work, the nature of the solutions of the BTMU and BTML models for the free overfall problem were examined. Detailed description of the numerical simulation procedures for this flow problem (based on the proposed models) can be found in Zerihun and Fenton [20]. For this simulation problem, the origin of the coordinate system was set at the brink section.

The computed flow surface profiles for subcritical approach flow are compared with the experimental results in Fig. 10. Upstream of the brink section, the results of both models agree well with the experimental data. Although the observation was taken for a short length of the flow domain, the BTMU model simulates the upper nappe profile of the jet more accurately than the BTML model. The BTML model result starts to deviate from the measured data for this part and shows relatively steep water surface slope at the brink section. For this flow situation, the brink depth is an important parameter for estimating the flow rate. This depth is predicted very well by the BTMU model with an error of only 2.6%.

Fig. 11 plots the non-dimensional pressure distribution upstream of the overfall, p/p_0, versus the non-dimensional height above the bed, h_s/H for both numerical and experimental cases. It can be seen that the result of the BTMU model shows atmospheric pressure right across the brink section due to the pre-assumed constant centrifugal term at a vertical section. Contrary to this, the BTML model predicts

Fig. 9. Comparison of predicted and measured flow profiles for transcritical flow over a hump with lateral contraction.
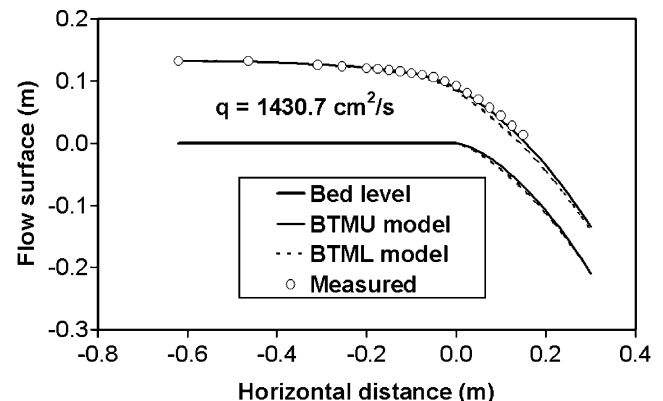

Fig. 10. Comparison of predicted and measured flow profiles in a free overfall ($Fr_0 = 0.95$).
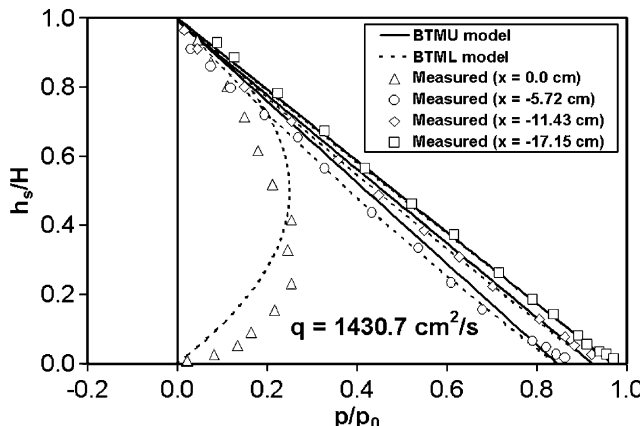
Fig. 11. Comparison of predicted and measured pressure profiles ($Fr_0 = 0.95$).

the maximum pressure at the end section accurately, with an error of only 2%. However, it indicates some deviation for the location of the maximum pressure, about 27% of H. In general, the prediction of the pressure distribution profile using the BTML model is satisfactory and follows a similar pattern to the observed values. Also, this model predicts the pressure distributions more accurately at vertical sections, 5.72 cm and 11.43 cm to the left of the brink section, where the flow has considerable streamline curvature. At a distance of 17.15 cm from the end section, the curvature of the streamline is negligible; both models provide similar results which agree very well with the experimental data. This comparison suggests that a higher-order pressure equation should be used for accurate simulation of the pressure distribution of a flow with pronounced curvature of streamlines.

For all simulation cases, both models required almost equal simulation run-time to converge to a final solution starting from the assumed initial position of the free surface. A typical computational time for the problem of flow in a channel with curved bed and sidewall was 18 s and 20 s respectively for the BTML and BTMU models using a Pentium-IV 2.0 GHz based personal computer.

As already indicated, the assumed distribution shapes of the centrifugal term determine the degrees of the resulting corrections for the effect of the non-hydrostatic pressure distribution. The overall simulation results of this study demonstrate that the proposed approximations for these corrections have only a marginal effect on the predictions of flow surface and bed pressure profiles. However, the pressure distribution simulation results of the considered flow problems are very sensitive to these approximations.

6. Summary and conclusions

Two one-dimensional Boussinesq-type momentum equation models, which incorporate different degrees of correction for the effects of the curvature of the streamline, were investigated for simulating transcritical flows at short length transitions in open channel flow measuring structures. These models—the Boussinesq-type momentum

equation uniform (BTMU) model and the Boussinesq-type momentum equation linear (BTML) model—were developed based on the assumptions of uniform and linear variation of the centrifugal term at a vertical section. Finite difference approximations were employed to discretise the flow equations. The Newton–Raphson iterative method with a numerical Jacobian matrix was used for the solution of the resulting non-linear algebraic equations. The models then simulated different test cases for flows in channels with predominant non-hydrostatic pressure distribution effects. Comparison of the numerical prediction results with experimental data was also presented.

Generally speaking, good agreement was observed between the predicted and measured data. Results of this investigation reveal that the 2-D flow structure for the transcritical flow situations are better described by the BTML model. The results also demonstrate the superior performance of the current computational scheme compared to a previous scheme based on the shooting method for the solutions of such equations. This study suggests that a higher-order pressure equation should be used when accurate simulation of the pressure distribution of a flow with pronounced curvatures of streamlines is sought.

References

[1] Bickley WG. Formulae for numerical differentiation. Math Gaz 1942;25:19–27.
[2] Bos MG. Discharge measurement structures. Wageningen: ILRI; 1978.
[3] Boussinesq J. Essai sur la théorie des eaux courantes. Mémories Présentés par Divers Savants à l'Académie des Sciences, Paris 1877;23(1):1–680.
[4] Dressler RF. New nonlinear shallow flow equations with curvature. J Hydraul Res 1978;16(3):205–20.
[5] Fenton JD. Channel flow over curved boundaries and a new hydraulic theory. In: Proceedings of the 10th Congress, APD-IAHR, Langkawi, Malaysia 1996;2:266–73.
[6] Fletcher CAJ. Computational techniques for fluid dynamics, 1. Berlin Heidelberg, Germany: Springer-Verlag; 1991.
[7] Hager WH, Hutter K. Approximate treatment of plane channel flow. Acta Mech 1984;51:31–48.
[8] Hager WH. Equation of plane, moderately curved open channel flows. J Hydraul Eng-ASCE 1985;111(3):541–6.
[9] Khafagi A. Der venturikanal: Theorie und anwendung. Eidgenössiche Technishe Hochschule Zürich, Mitteilungen der Versuchsanstalt für Wasserbau und Erdbau, Zürich, 1942.
[10] Khan AA, Steffler PM. Vertically averaged and moment equations model for flow over curved beds. J Hydraul Eng-ASCE 1996;122(1):3–9.
[11] Khan AA, Steffler PM. Modelling overfalls using vertically averaged and moment equations. J Hydraul Eng-ASCE 1996;122(7):397–402.

[12] Law AWK. Single layer flow over an obstacle consisting of a contraction and sill. Hydraulic Engineering Laboratory Report No. UCB/HEL-85/06, Department of Civil Engineering, University of California at Berkeley, 1985.

[13] Law AWK. Steady flow over an obstacle with contraction and sill. In: Proceedings of the 27th Congress, IAHR, San Francisco, 1997. p. 787–92.

[14] Matthew GD. Higher order, one-dimensional equations of potential flow in open channels. Proc Instn Civ Eng, London, England 1991;91:187–201.

[15] Rajaratnam N, Muralidhar D. Characteristics of the rectangular free overfall. J Hydraul Res 1968;6(3):233–58.

[16] Ranga Raju KG, Srivastava R, Porey PD. Scale effects in modelling flows over broad-crested weirs. J Irrig Power 1990;47(30):101–6.

[17] Sivakumaran NS, Hosking RJ, Tingsanchali T. Steady shallow flow over curved beds. J Fluid Mech 1983;128:469–87.

[18] Steffler PM, Jin Y. Depth averaged and moment equations for moderately shallow free surface flow. J Hydraul Res 1993;31(1):5–17.

[19] Ye J, McCorquodale JA. Depth-averaged hydraulic model in curvilinear collocated grid. J Hydraul Eng-ASCE 1997;123(5):380–8.

[20] Zerihun YT, Fenton, JD. Boussinesq-type momentum equations solutions for steady rapidly varied flows. In: Proceedings of the 6th international conference on hydro-science and engineering, Brisbane, Australia 2004, CD-ROM.